CHAPTER 4

Earthquake Loss Estimations

This chapter provides an overview of the earthquake loss estimations. Nine topics will be discussed in this chapter: (1) Building Classification, (2) Soil Classification, (3) Attenuation Relationship, (4) Assumed Earthquake Event, (5) Peak Ground Acceleration, (6) Building Losses (Complete Level), (7) Human Losses, (8) Building Damage after Rehabilitation and (9) Human Losses after Rehabilitation.

4.1 Building Classification

This section shows the results of buildings in the area with screening phase RVS method was used to inspect each building in Chiang Rai Municipality (79.3 sq.km., 46,775 units) and classified both in term of their use, and structural system. Figures 4.1 – 4.11 show the example building in the area with different types of buildings materials. Figure 4.12 shows the RVS final score of buildings in the surveyed area.

Figure 4.1 Concrete moment resisting frame (C1)

Figure 4.2 Concrete shear Wall (C2)

Figure 4.3 Concrete frames with unreinforced masonry infill (C3)

Figure 4.4 Steel moment – resisting frame (S1)

Figure 4.5 Steel braced frame (S2)

Figure 4.6 Light metal frame (S3)

Figure 4.7 Light wood frame building, Area ≤ 464.5 sq.m. (W1)

Figure 4.8 Wood frame building, Area > 464.5 sq.m. (W2)

Figure 4.9 Concrete frames with unreinforced masonry infill with light metal frame (S3C3)

Figure 4.10 Concrete frames with unreinforced masonry infill with light wood frame building, Area ≤ 464.5 sq.m. (W1C3)

Figure 4.11 Concrete frames with unreinforced masonry infill with wood frame building, Area > 464.5 sq.m. (W2C3)

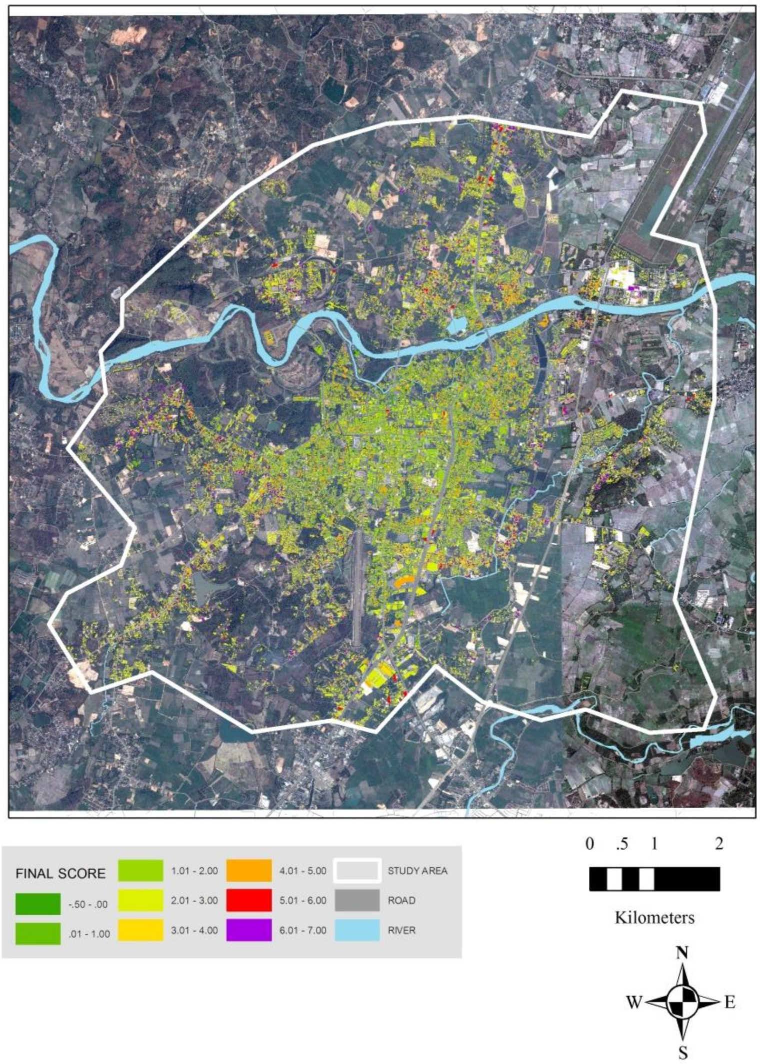

Figure 4.12 Final score from Rapid-Visual Screening Method

Table 4.1 Summary of final score (S) score in the study area

RVS Final Score (S)	Damage Potential	Units
S<0.3	High probability of Grade 5 damage; Very high probability of Grade 4 Damage	58
0.3<S<0.7	High probability of Grade 4 damage; Very high probability of Grade 3 Damage	13
0.7<S<2.0	High probability of Grade 3 damage; Very high probability of Grade 2 Damage	18,449
2.0<S<2.5	High probability of Grade 2 damage; Very high probability of Grade 1 Damage	4309
S>2.5	Probability of Grade 1 damage	23,946

Table 4.1 shows the summary of final score in the surveyed area. The final score is related to probability of the building will collapse. The study area has final score less than 2 about 39.59%, suggesting that the buildings are vulnerable and need details analysis. It implies that there is a chance of 1 in 100 (a 1% chance of collapse) these the buildings will collapse if such ground motions occur.

It can therefore been said that most buildings in Chiang Rai have been designed without consideration of the seismic effect. Therefore, a Pre-seismic design level was assumed for the analysis. Table 4.2 shows the structural type of buildings in Chiang Rai city. The structural type was defined according to NEHRP Handbook for the Seismic Evaluation of Buildings – A Pre-standard (FEMA 310, 1998). Most of them were classified as C3 or Low-rise reinforced concrete frames with unreinforced masonry, infilled walls and within the building category type of residential.

Table 4.2 Structural type of buildings in the study area

Building Type	Structural Type											Grand Total
	C1	C2	C3	S1	S2	S3	URM	W1	W1C3	W2	W2C3	
Assembly	9		38	2								49
Commercial	122	160	5,515	17	12	10		126	49	8	3	6,022
Emer. Services	12	10	223					5				250
Government	28	4	622	3				42	6	6		711
Historic	21		301				24	18	58		7	429
Hotel	2	24	185	1				1	1	3		217
Industrial	48	1	348	19	8	12		15	7	2		460
Office	20	18	277	6		1	1	2	7			332
Other	116		2,180	9	1	3	5	146	29	2		2,491
Residential	1,140	86	30,372	79	9	5	4	2,155	1,193	201	6	35,250
School	25	26	434					3	62	1	13	564
Grand Total	1,543	329	40,495	136	30	31	34	2,513	1,412	223	29	46,775

where;

C1	is concrete moment-resisting frame buildings
C2	is concrete shear-wall buildings
C3	is concrete frame buildings with unreinforced masonry infill walls
S1	is steel moment-resisting frame buildings
S2	is braced frame buildings
S3	is light metal buildings
URM	is unreinforced masonry bearing-wall buildings
W1	is light wood-frame buildings smaller than or equal to 464.52 sq.m. (or 5,000 sq.ft.)
W2	is light wood-frame buildings larger than 464.52 sq.m. (or 5,000 sq.ft.)
W1C3	is combination structure light wood-frame and concrete frame buildings with unreinforced masonry infill walls smaller than or equal to 464.52 sq.m. (or 5,000 sq.ft.)
W2C3	is combination structure light wood-frame and concrete frame buildings with unreinforced masonry infill walls larger than 464.52 sq.m. (or 5,000 sq.ft.)

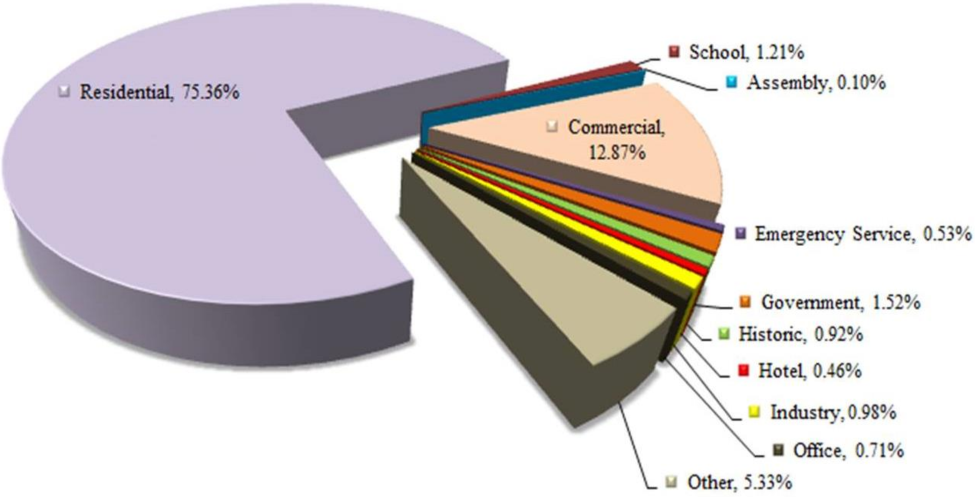

Figure 4.13 Proportion of the buildings in the study area

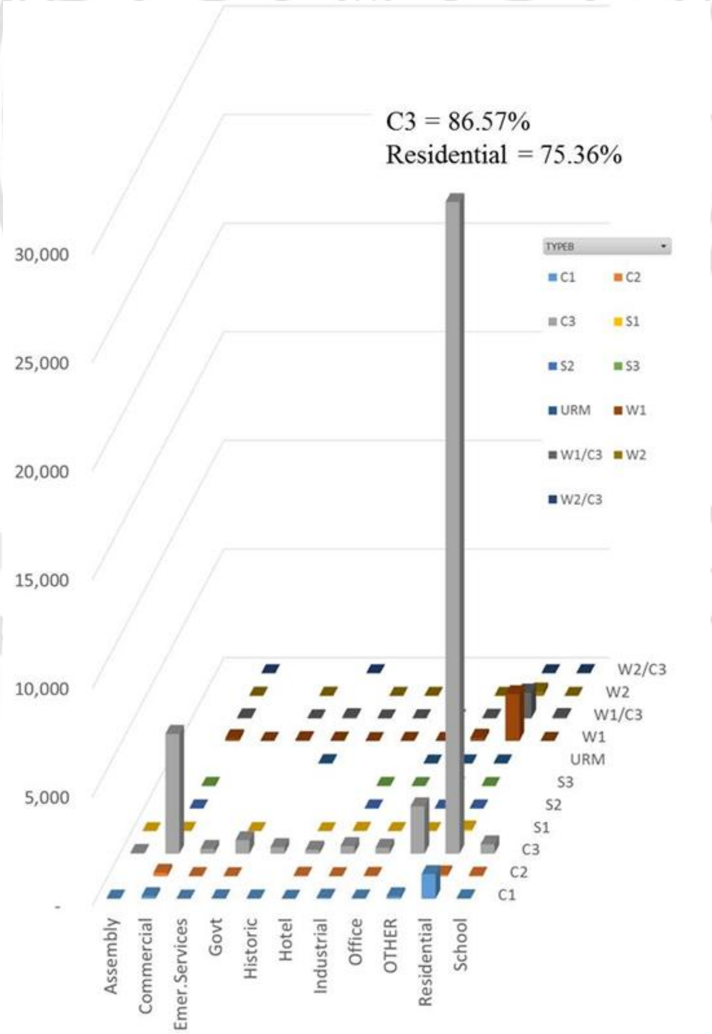

Figure 4.14 Classification of buildings in the study area

Figures 4.15 - 4.17 show the spatial distribution of building's category, structure type of buildings and distribution density of buildings, respectively.

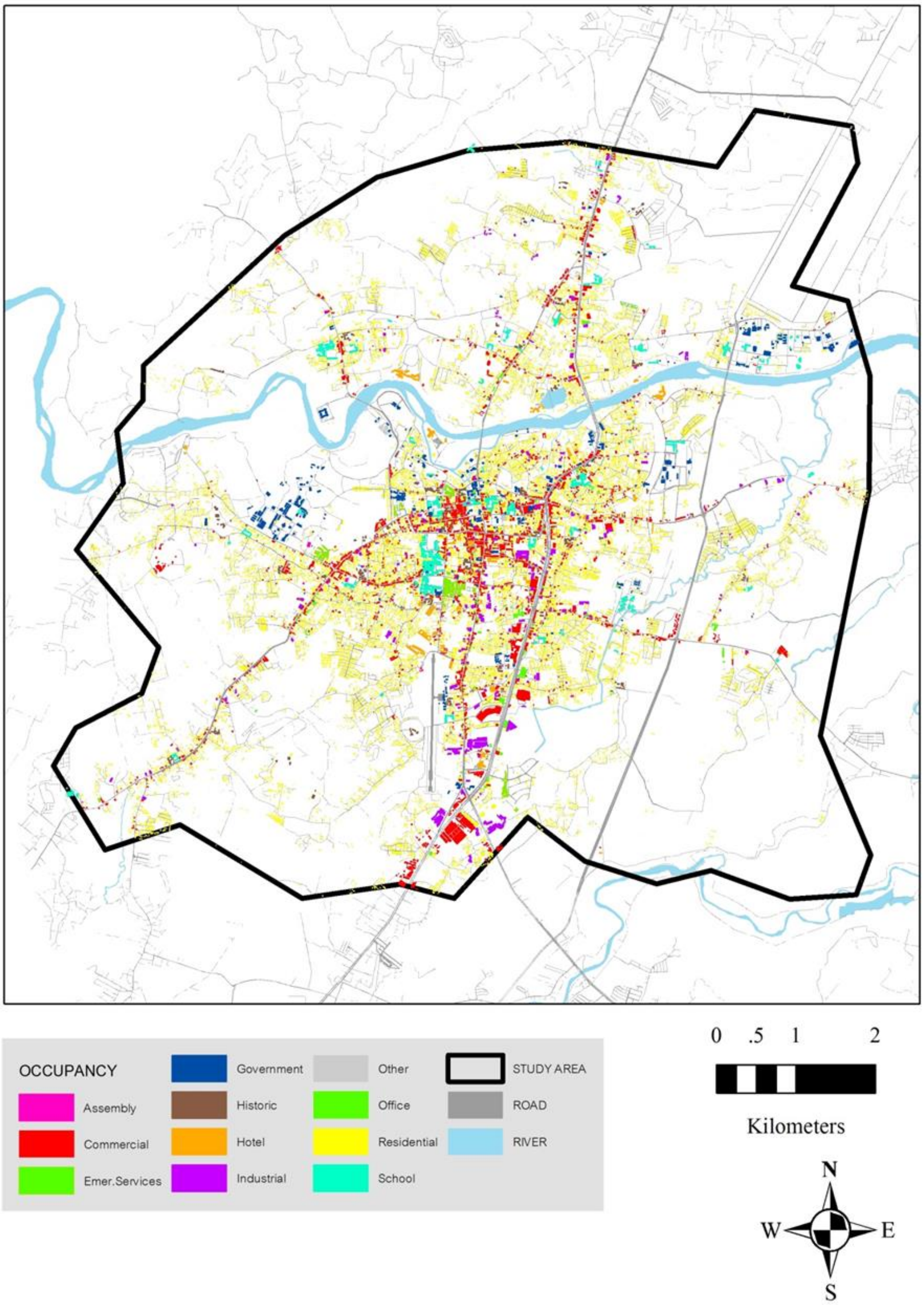

Figure 4.15 Distribution of building type

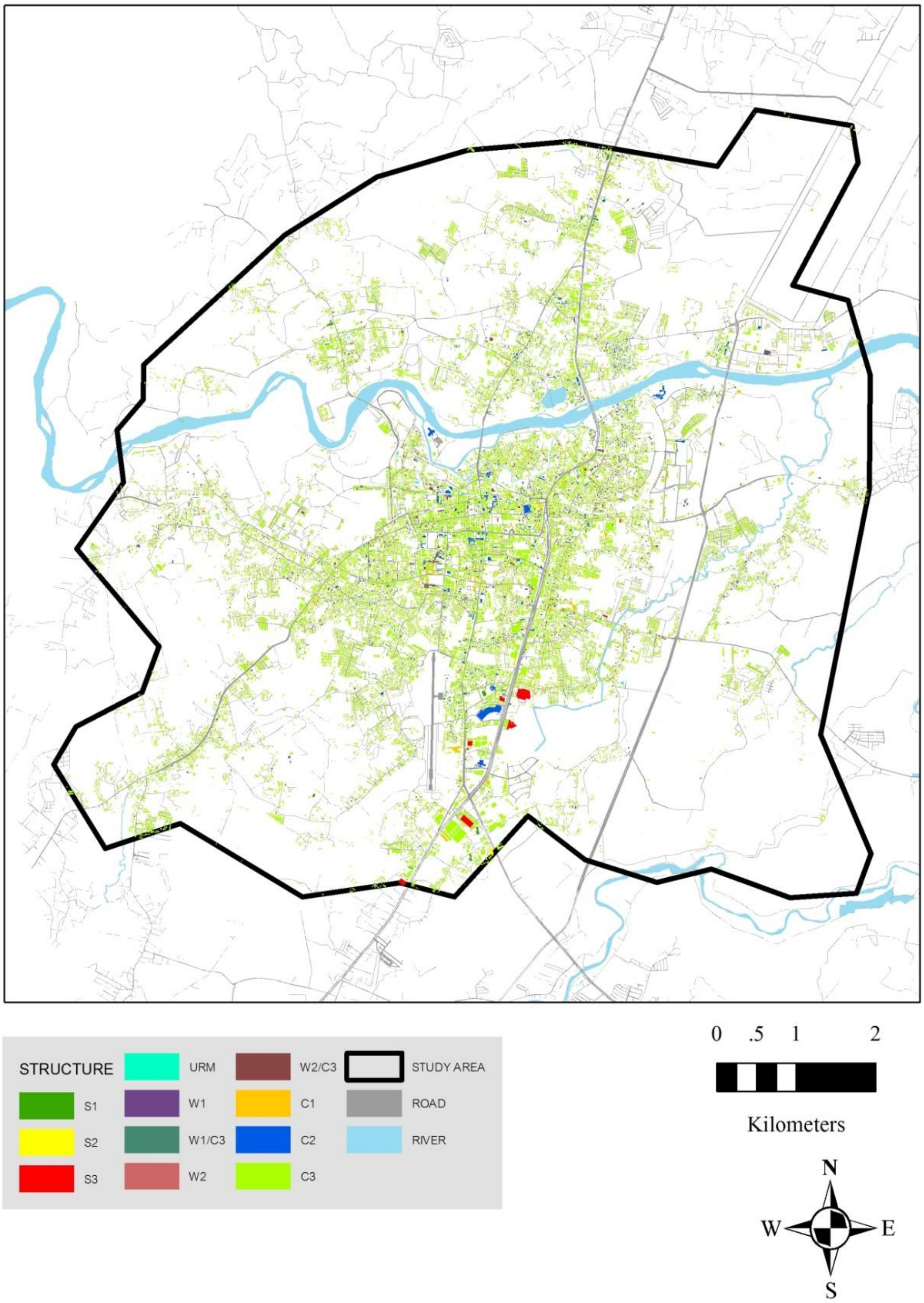

Figure 4.16 Distribution of structural type of buildings

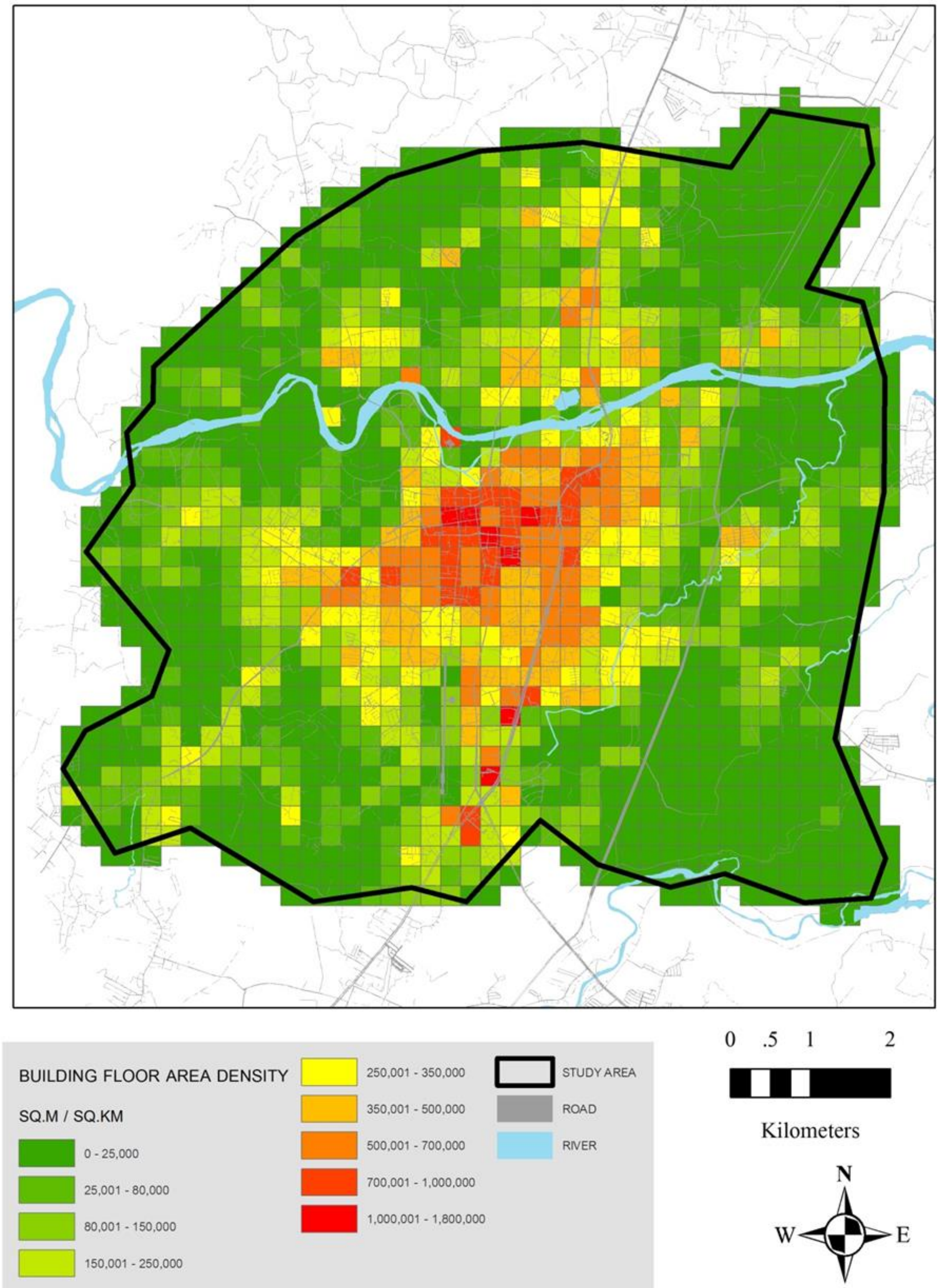

Figure 4.17 Distribution density of buildings (sq.km.)

4.2 Soil Classification

The ground motion at a specific site may be amplified through it's soil profile, depending on the soil conditions. By using shear velocity, the soil conditions at a site can be classified as A through F, as seen in Table 4.3.

Table 4.3 Site classification according to the NEHRP provisions (FEMA 222A, 1997)

Site Class	Site class description of 1997 UBC Provisions	Shear-wave velocity, (m/s)
A	Hard rock, eastern United States site only	> 1500
B	Rock	760 - 1500
C	Very dense soil and soft rock; Undrained shear strength $u_s \geq 2000$ psf ($u_s \geq 1000$ kPa) or $N \geq 50$ blows/ft.	360 - 760
D	Stiff soild; Stiff soil with undrained shear strength 1000 psf$\leq u_s \leq$2000 psf (50 kPa $\leq u_s \leq$100 kPa), or $15 \leq N \leq 50$ blows/ft.	180 - 360
E	Soft soils; Profile with more than 10ft (3m.) of soil clay defined as soil with plasticity index PI > 20, moisture content w > 40% and undrained shear strength u_s < 1000 psf (50kPa), or N < 15 blows/ft.	< 180
F	Soils requiring site specific evaluations. 1) Soil vulnerable to potential failure or collapse under seismic loading: e.g. liquefiable soils, quick and highly sensitive clays, collapsible weakly cemented soils. 2) Peats and/or highly organic clay 10ft (3m.) or thicker layer. 3) Very high plasticity clays: 25ft (8m.) or thicker layer with plastic index > 75 4) Very thick soft/medium stiff clays: 120ft (36m.) or thicker layer.	n.a.

In this study, based on the soil investigations by Standard Penetration Test (SPT). The SPT average values $\overline{N}$ can be determined as follows:

$$\overline{N} = \frac{\sum_{i}^{m} t_i}{\sum_{i}^{m} (t_i / N_i)} \tag{4.1}$$

Where;

t_i is Thickness of soil layer *i*

N_i is Number of times of SPT test in soil layer *i*

It can be seen from Table 4.4 and appendix that most of the area can be classified as D class or stiff soil with the shear velocity between 180 and 360 m/sec, which was used in the analysis.

Table 4.4 Summary of soil investigated data

No.	Description	$\overline{N}$
1	BH.1	20.32
2	BH.2	13.72
3	BH.3	17.76
4	BH.4	18.51
5	BH.5	14.63
6	BH.6	15.01
7	BH.7	20.21
8	BH.8	16.06
9	BH.9	19.89
10	BH.10	12.30
11	BH.11	21.80
12	BH.12	14.72
13	BH.13	13.39
14	BH.14	15.77
15	BH.15	14.45
Average		16.57

4.3 Attenuation Relationship

Attenuation laws are typically used to determine the level of earthquake intensity at the bed rock depth for the considered sites. Through the attenuation model, the peak ground acceleration, velocity or displacement at the considered sites can be estimated. Although, currently, numerous attenuation laws have been published and available to use, the one that is most appropriate for the site conditions and ground motion type must be carefully selected. In this study, based on the fault moving mechanism, the earthquake intensity for the study area was estimated through the attenuation model as proposed by Youngs *et al*. (1997). The young's attenuation relationship was expressed in detail as mention below;

$$\begin{aligned}\ln(SD) = {} & A_{IF}G_{IF} + A_{IS}G_{IS} + 1.414M + b(10-M)^{3} + c\ln(R + 1.782e^{0.554M}) \\ & + 0.00607H\end{aligned} \qquad (4.2)$$

Where;

SD	=	Average peak ground acceleration or spectrum acceleration
M	=	The Earthquake magnitude (Mw, Moment magnitude)
R	=	Sources (epicenter) to site distant (km.)
A_{IF}, A_{IS}	=	The multiplication factor for the mechanism of the earthquake generation which is interface or intraslab, as show in Table 4.5
G_{IF}, G_{IS}	=	Source Type, 0 for interface, 1 for interslab

The values of A_{IF}, A_{IS} are given in Table 4.5 from site-specific property of earthquake mechanism types. And the range of applicability is 0 to 200 km. for distance.

Table 4.5 Multiplication factor for the mechanism of the earthquake

Period	A_{IF}	A_{IS}	b	c
PGA	0.2418	0.6264	0.0	-2.552
0.3	0.4878	0.8724	-0.0036	-2.454
1.0	-1.494	-1.1096	-0.0064	-2.234

4.4 Assumed Earthquake event

For the study area, an earthquake event was considered for loss estimation with an epicenter magnitude of 5 and 10 km. depth as shown in Figure 4.18. The earthquake is on Mae Lao fault line, which is located 3.71 km away from downtown to the north-west of Chiang Rai Municipality. According to the past records, earthquakes have occurred in the selected location (epicenter coordination is latitude 19.9294491406158, longitude 99.7990874774044 or 583628N, 2203873E).

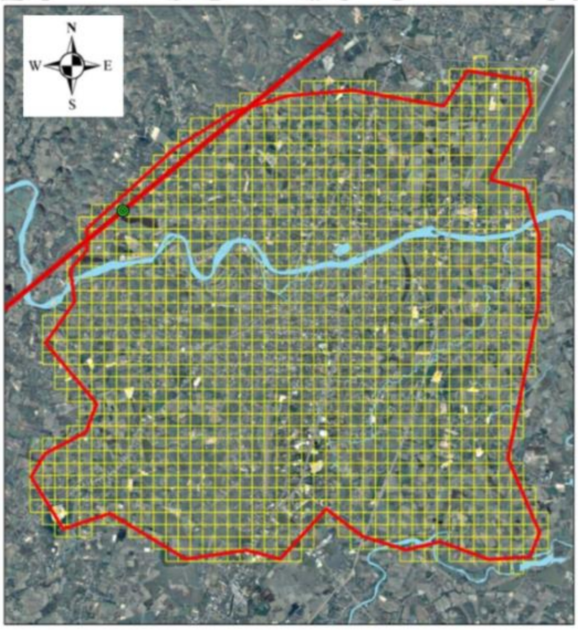

Figure 4.18 Epicenter of the assumed earthquake with magnitude of 5

4.5 Peak Ground Acceleration

For the assumed earthquake event and the attenuation model, Figure 4.19 shows the peak ground acceleration contour for the study area. The acceleration was in the range of 0.104 g to 0.241 g in the earthquake scenario, which is in the same intensity range as the past research in the area (Warnitchai *et al.*, 2000).

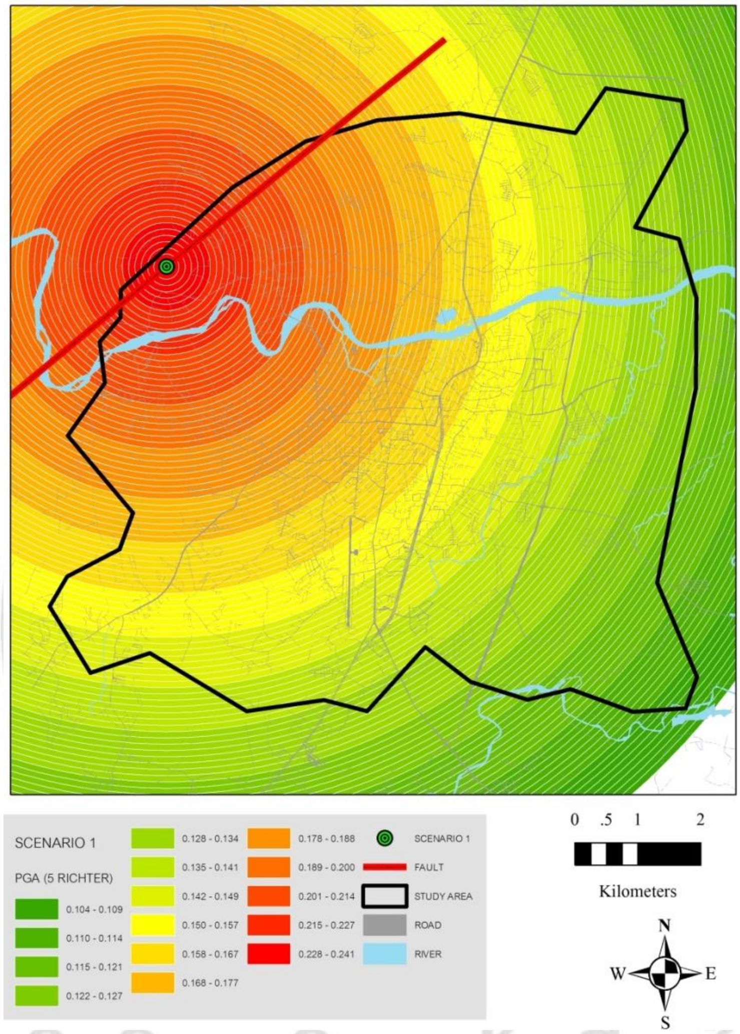

Figure 4.19 Peak ground acceleration contour

4.6 Building Losses (Complete Level)

For the building losses estimate, the capacity spectrum method essentially involves comparison of the capacity of a structure, represented by the capacity spectrum, with the seismic demand represented by an acceleration displacement response spectrum. The performance point of a model building type is obtained from the intersection of a capacity spectrum and demand spectrum. The performance is then input into fragility curves, which allow the probability of exceeding a number of damage states, given this performance point. The vulnerability relationships refer to structural damage state defined (essentially on the basis of displacement drifts) as slight, moderate, extensive, and complete (Erdik *et al.*, 2011). The number of casualties is due to direct structural damage for any structure type. The estimates are based on loss of life that occurred on probability of collapse given a complete damage state. Figure 4.20 shows the distribution of the complete damage (collapse) of the buildings in Chiang Rai Municipality when subjected to the earthquake scenario. It illustrates that the maximum damage occurred at the central part of the study area with a complete damage area of about 2,633,947.92 sq.m. (400,000 sq.m. in every 1 sq.km.) or 24.79% of the entire building area.

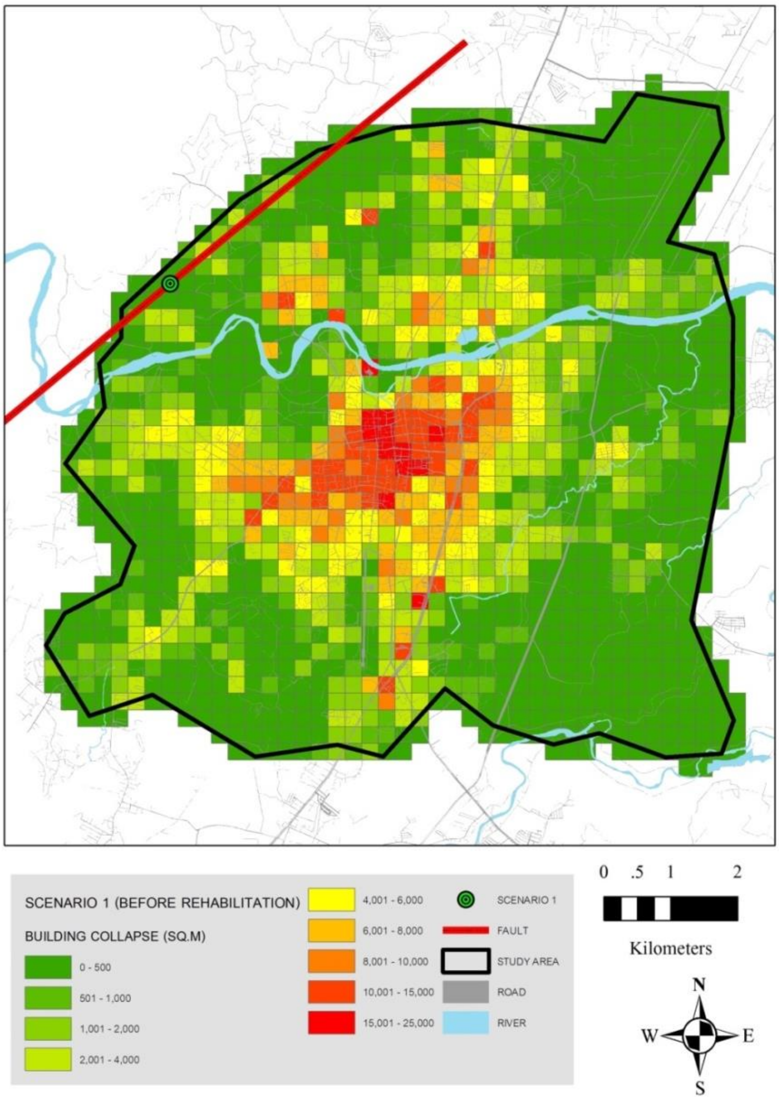

Figure 4.20 The complete damage (collapse) of the buildings

4.7 Human Losses

The numbers of human deaths were calculated for two the different times as shown in Figures 4.21 – 4.22. The level of severity of instantaneously killed was about 712 persons during the night time, and 1,027 persons during the day time, equivalent to 0.365 and 0.371 percent for the night time and day time, respectively, corresponding to the total number of people living in the buildings.

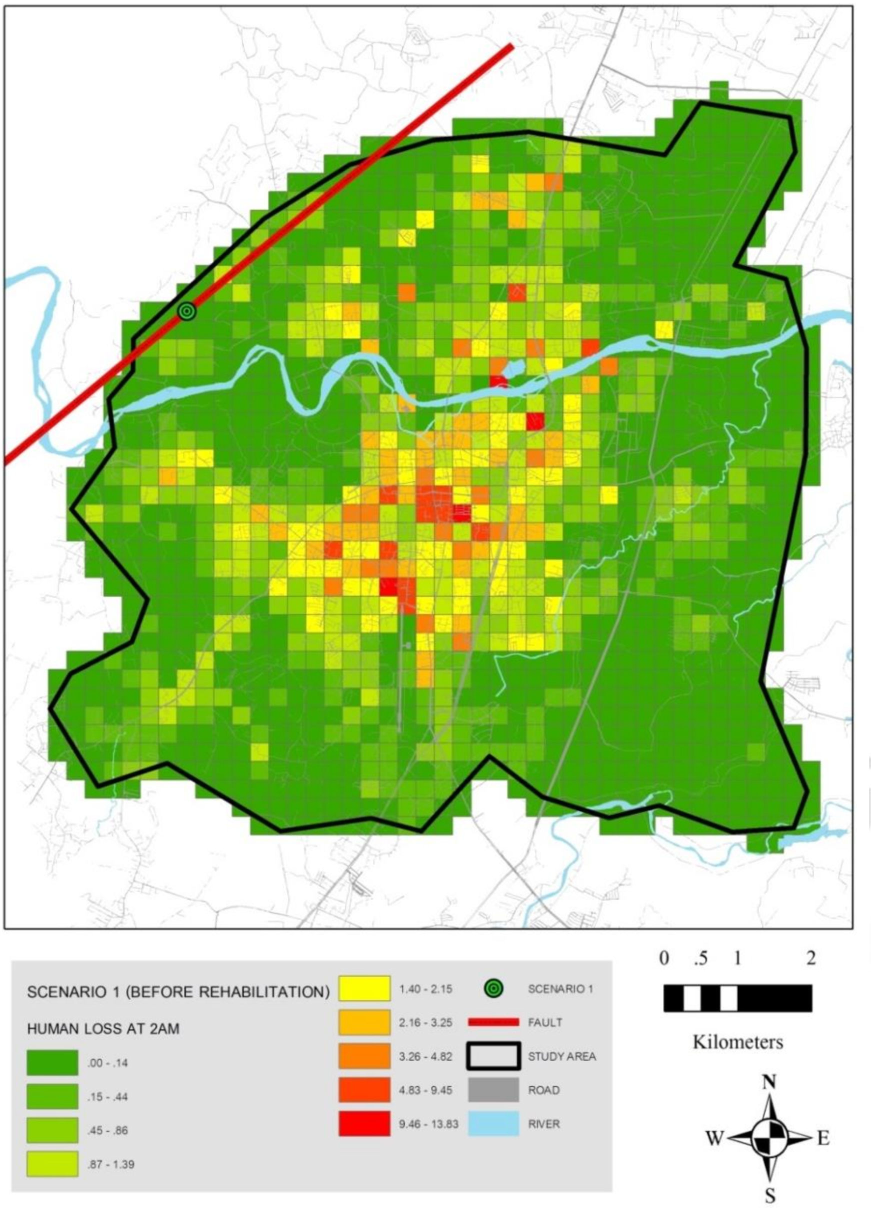

Figure 4.21 Distribution of human casualties in night time (2:00 AM)

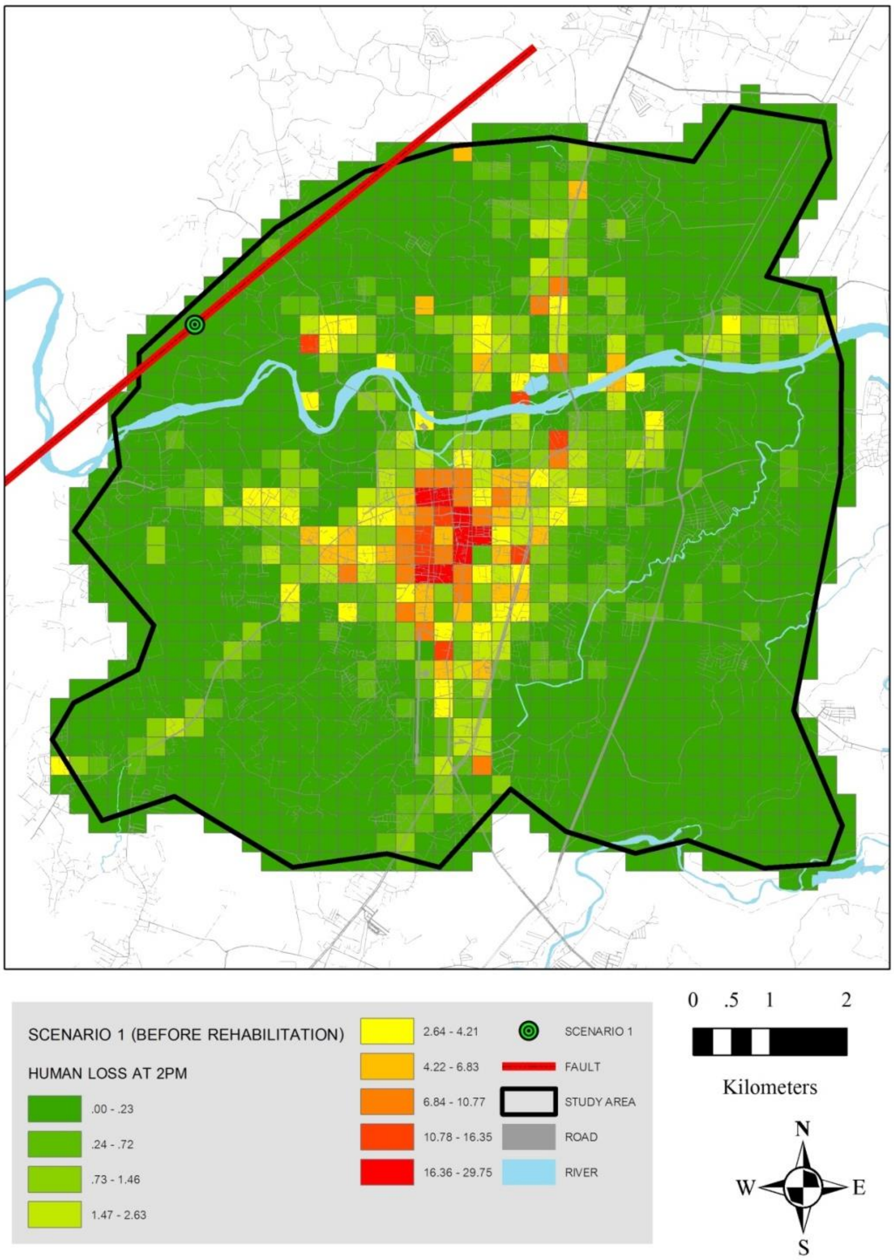

Figure 4.22 Distribution of human casualties in day time (2:00 PM)

4.8 Building damage after rehabilitation

Figure 4.23 shows the distribution of the building damage after rehabilitation of the selected buildings. The selected important buildings compose of 564 school buildings, 96 hospital buildings, 154 emergency services buildings and 711 government offices. The complete damage of those buildings, before the rehabilitation, covered about 225,587.35 sq.m., which was reduced to about 115,043.34 sq.m. after rehabilitation to a moderate seismic design level standard. The reduction of the damage area can account more than 49%. Overall, it illustrates that the complete damage area was reduced from 2,633,947.92 sq.m. to 2,440,244.88 sq.m. or 7.35% of the entire building area.

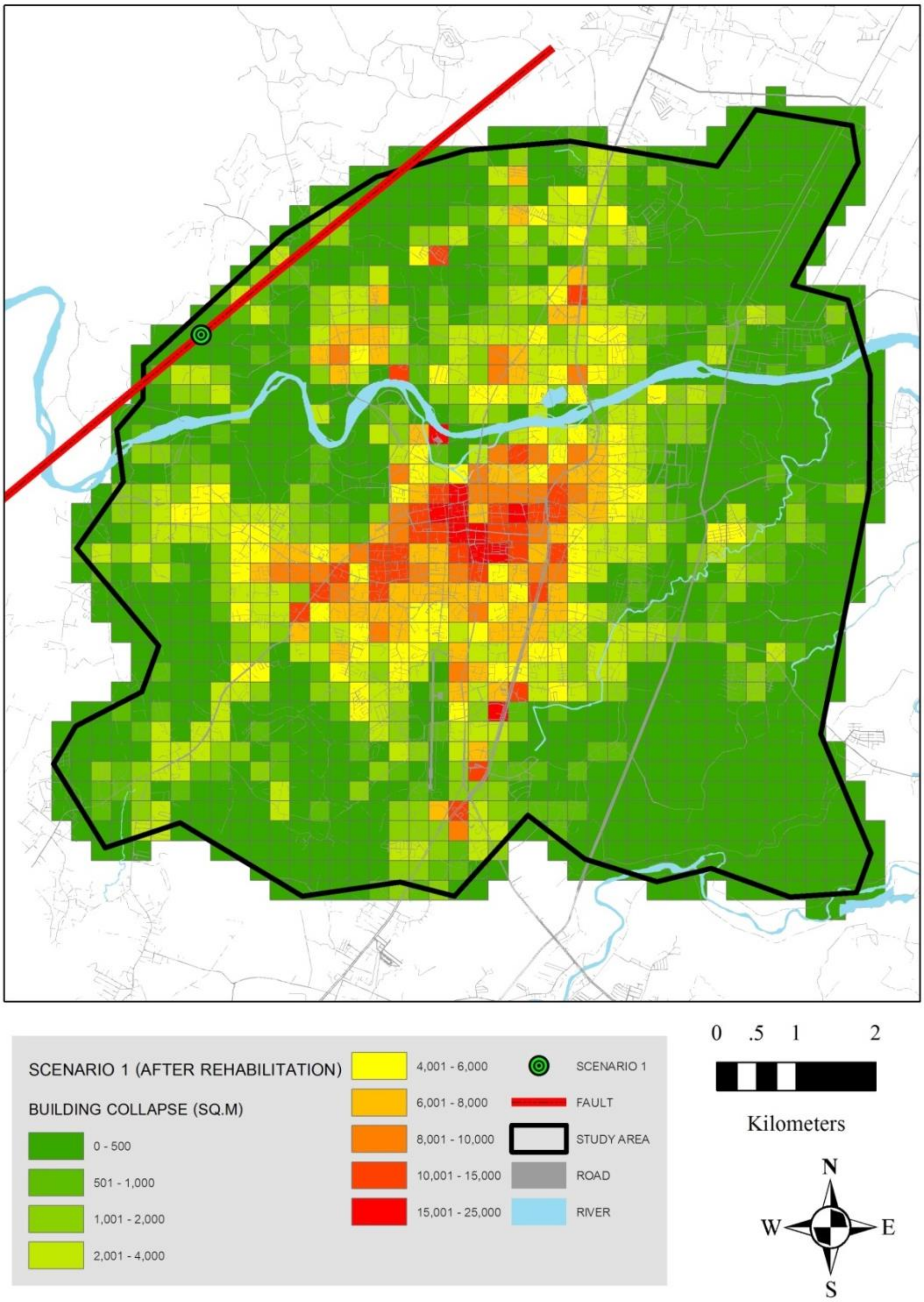

Figure 4.23 The complete damage after rehabilitation

4.9 Human Losses after rehabilitation

As the upgrading lead to less building damage, the number of casualties was also reduced accordingly. However, with a limitation on budget and time, incremental upgrading focusing on important buildings has been generally considered. For this study, the numbers of human fatalities in the upgraded buildings were reduced from 4 deaths before to 1 death after the rehabilitation during the nighttime. It is evident that in the daytime, with high occupancy, the numbers of deaths were reduced from 295 persons to 86 persons after the rehabilitation. In proportion, the reduction in the numbers of deaths was about 75% for the nighttime and 70.85% for the daytime. Table 4.6 shows the number of people and deaths before and after the rehabilitation of important buildings

Table 4.6 Number of people and deaths before and after rehabilitation

Important level	Building Occupancy	Population		Losses Before Rehab.		Losses After Rehab.	
		2:00 AM	2:00 PM	2:00 AM	2:00 PM	2:00 AM	2:00 PM
Highly Important	Hospital & Emergency Services	430	20,883	2	80	0.5	24
	Government Offices	499	24,253	2	86	0.5	23
	Schools	0	33,957	0	129	0	39
	Sub-Total	929	79,093	4	295	1	86
Less Important	Other Buildings	194,265	197,595	708	732	708	732
	Grand Total	195,194	276,688	712	1,027	709	818

Figures 4.24 – 4.25 show the numbers of human deaths after the rehabilitation of existing structures for the two different times. In the study area, human casualties were instantaneously killed 709 and 818 persons, approximately for night time and day time, respectively.

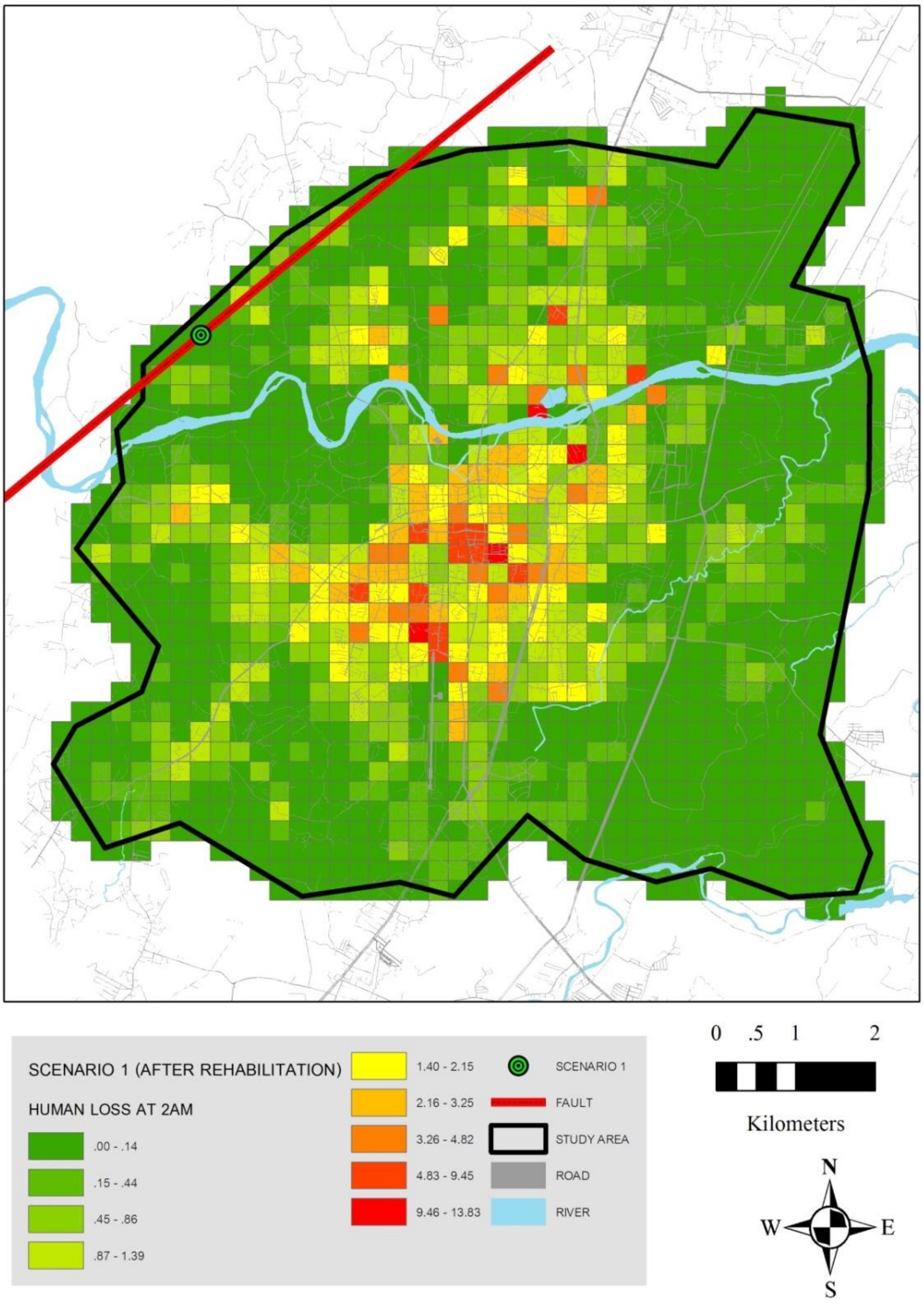

Figure 4.24 Distribution of human casualties after rehabilitation of existing structures in night time 2:00 AM

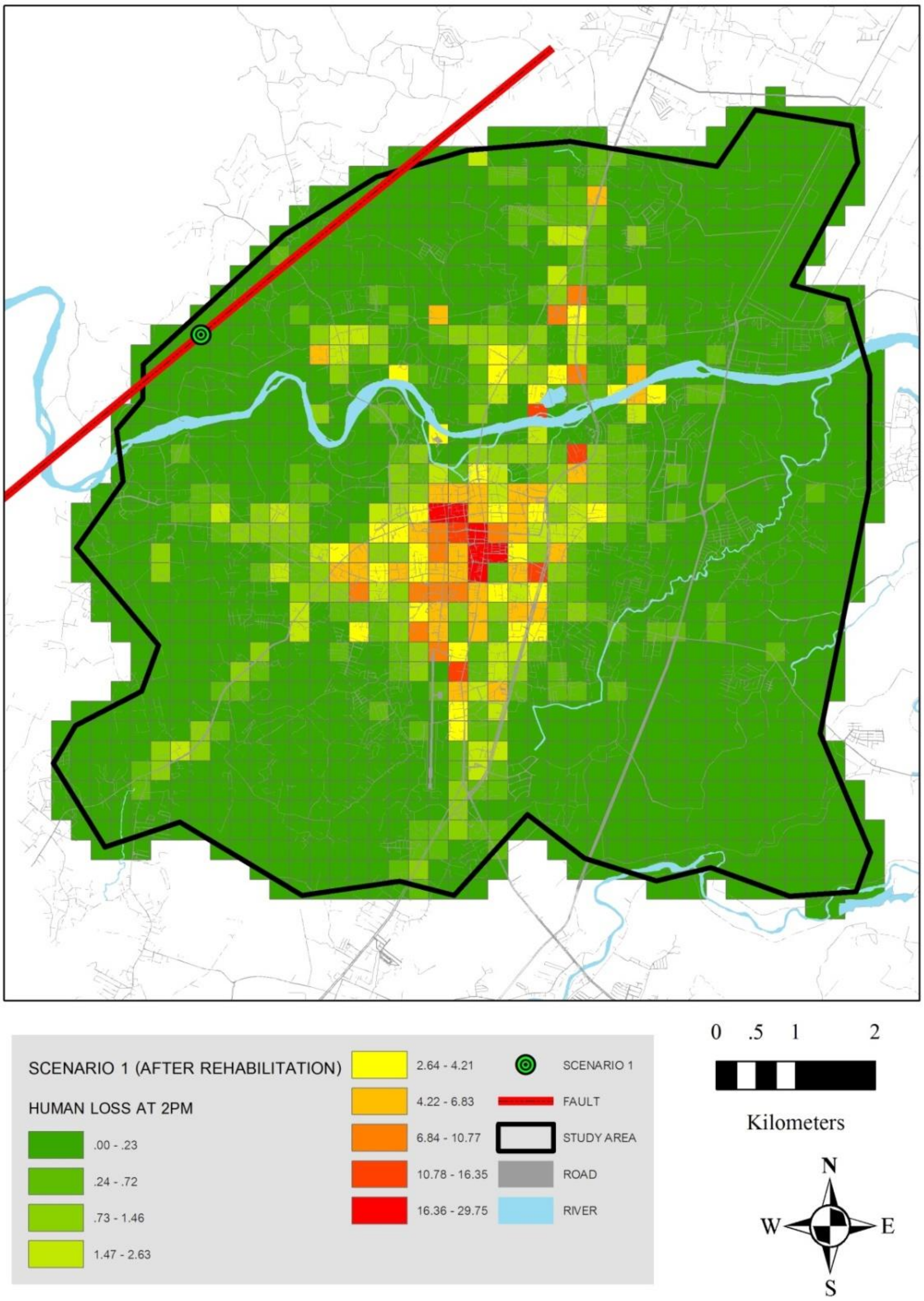

Figure 4.25 Distribution of human casualties after rehabilitation of existing structures in day time 2:00 PM